

Spectral Estimates of the Troposphere Using Least Squares and Maximum Likelihood

S. J. Wellard

Abstract—Given the significant cost and effort required to field infrared sensors capable of cutting-edge performance, each step of the development process, from experiment concept to calibrated sensor, must be optimized to insure maximum quality in the final processed data. This is particularly important if the final data is to be used as a basis for decisions about the properties of future sensors or for claims about the characteristics of the Troposphere.

The spectra estimation process depends critically on how well the technique anticipates and models the operational properties of the system, how well the optical and electrical characteristics of the system are characterized, how closely the temporal properties of the system approximate a linear, time-invariant system, and how well system noise characterization are factored into the process that ends with quality spectra. To this end an alternate spectrum estimation algorithm, Expectation Maximum inversion (EM), is investigated and compared against the standard Fast Fourier Transform (FFT) operating on data collected during the flight of the spectrometer developed for the Far Infrared Spectroscopy of the Troposphere (FIRST) program. A discussion of the characteristics of the FFT and EM transform is given along with some preliminary results.

Index Terms—Spectrometer, Interferometer, Fast Fourier Transform, Maximum Likelihood Spectral Estimation.

I. INTRODUCTION

Data processing is a critical step in an infrared spectrometer sensor program. Infrared sensor programs start with a sensor concept and then moved through design, fabrication, test, and calibration, to field operations where raw data is collected and stored for later transfer to data processing computers. This data is reduced to a final form with transforms and calibration information and delivered to scientists for analysis and validation. My research has focused on the spectral estimation processes that transform the spatial information of flight interferograms, recorded aboard a sensor platform, to final processed spectra ready for scientific review.

This paper describes an alternate spectral estimation technique, the Expectation Maximum (EM) algorithm, and compares some of its performance features against those of the traditional fast Fourier Transform (FFT).

II. FIRST SPECTROMETER DESCRIPTION

Manuscript received April 24, 2003.

S. J. Wellard is a doctoral candidate in the Electrical and Computer Engineering Department at Utah State University. The author can be reached at stan.wellard@sdl.usu.edu or swellard@cc.usu.usu.

The FIRST program, Far Infrared Spectroscopy of The Troposphere, was sponsored by the NASA-Langley Research Center in Hampton, Virginia. FIRST was conceived and developed as an NASA Instrument Incubator Program (IIP) [1] that seeks to gain confidence in the performance of new hardware before the hardware is designed into a satellite platform. The infrared sensor selected for this program was a Mickelson ‘porch-swing’ interferometer that has served as a standard instrument for the Space Dynamics Laboratory since the early 70s. FIRST was flown in New Mexico on a stratospheric balloon to demonstrate wide-band, high-throughput technology in a “similar-to-space” environment as required of an IIP. The sensor successfully demonstrated a measurement capability sufficient to give tropospheric scientists information about the spectral dependence of the radiation balance of the far-IR. Additionally, the sensor demonstrated its ability to do vertical temperature and moisture profiles. Information and data collected by satellite versions of FIRST would be used as inputs to global atmospheric weather models with emphasis on gaining insight into the causes and effects of global warming.

The FIRST interferometer was designed to cover a spectral range between 10 to 100 μm (1000 to 100 cm^{-1}) at 0.6 cm^{-1} spectral resolution. FIRST was developed to advance two technologies needed to provide measurements of the Earth’s spectral radiative energy budget. It successfully demonstrated the performance of a broad bandpass beamsplitter, and high throughput interferometer and optical system that could be radiatively cooled aboard a satellite in low earth orbit. The IID version provided calibrated measurements of the virtually unobserved far infrared (far-IR) portion of the Earth’s outgoing longwave radiation. Due to the budget limitations of the IIP program, FIRST was only tasked to improve the Technical Readiness Level (TRL) of interferometer, beamsplitter and optical system technologies from 4 to 6/10.

A schematic of a Mickelson interferometer is shown in figure 1 [2].

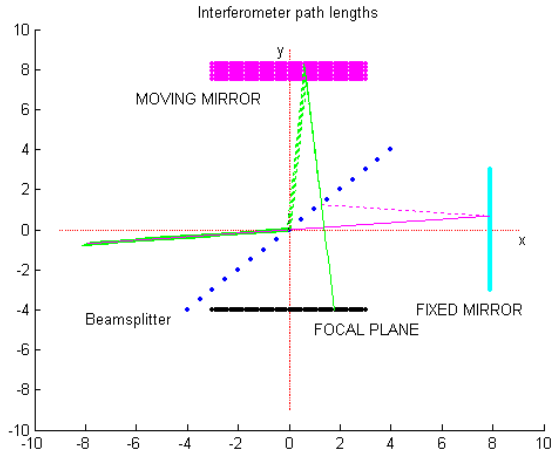


Figure 1: Basic Interferometer geometry showing incoming rays at an angle of 5 degrees.

This interferometer design has two circular mirrors oriented orthogonal to each other and displaced an equal distance from the center of the beamsplitter at the moving mirror’s rest position. Infrared energy enters the interferometer from the left at angles that range between 0 and 0.4 degrees and is divided by the beamsplitter. One-half of the energy reflects from the beamsplitter and goes to the moving mirror; the other half is transmitted through the beamsplitter to the fixed mirror.

Both halves are reflected back to the beamsplitter to be recombined constructively or destructively at the detectors dependent on the instantaneous path length difference between the two mirrors as the moving mirror are scanned, at a constant velocity, around its rest position. Half the energy originally input to the interferometer is reflected/transmitted back through the entrance aperture while the other half becomes useful signal at the focal plane.

The focal plane for FIRST was designed as a 10 X 10 array of circular detectors arranged in a square pattern making the sensor hyper-spectral. The detector for each was a micro-bolometer capable of covering the wide band-pass of the spectrometer. Each micro-bolometer was mounted at the focal point of a Winston cone flux concentrator. To allow the FIRST IIP sensor to mimic expected satellite-based focal plane designs, a sub-populated version was flown on FIRST with two detectors in each corner and two in the center. Detectors at the corners were used to confirm these areas could be properly illuminated by the optical system. Each scan of the moving mirror simultaneously produced 10 interferograms of the Troposphere or earth surface below the balloon gondola.

When the entrance aperture of the interferometer is illuminated by a quasi-monochromatic point source at wavenumber ($\sigma(i)$), representing a line in the spectral

domain, the resulting detector output will be given by the equation

$$E_{det} = 2rtB (\sigma)[1 + \cos(2\pi \sigma(i) x)d\sigma]. \quad (1)$$

The interferogram is defined as the second term in equation (1). This cosine function varies with x where x is the path difference $x_1 - x_2$. when other quasi-monochromatic point sources are added to the first, the interferogram is approximated by

$$I(x) = 2rt \sum_{i=1}^I B (\sigma(i))[\cos(2\pi \sigma(i) x) \quad (2)$$

The interferogram is now a complex waveform similar to the one shown in figure 2.

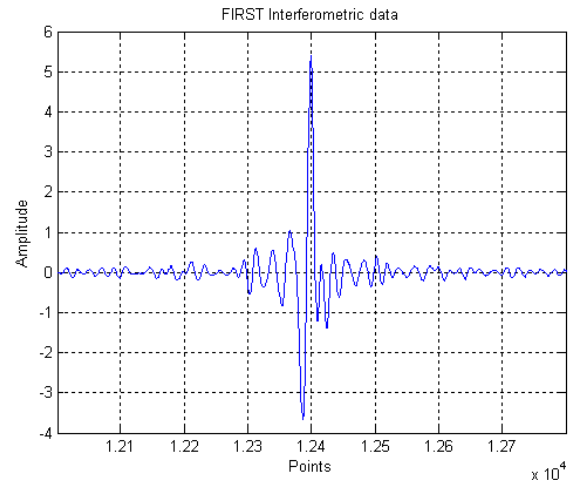


Figure 2: FIRST interferogram representative of approximately 15,000 collected during flight.

Once recorded interferograms are down-loaded, the transform process can begin. The Fast Fourier Transform (FFT), an optimized version of the Discrete Fourier Transform (DFT), has long been the first choice to perform the desired spectral estimates. Figure 3 shows examples of transformed, calibrated spectra.

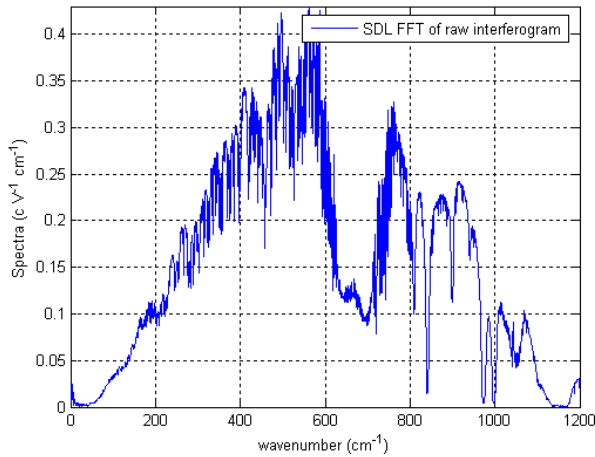


Figure 3: FFT transform of interferogram shown in figure 2. This is a view looking down into the Troposphere.

III. FFT “MULTIPLEX DISADVANTAGE”

While the FFT is a fast, effective least-squares spectral estimator, it does have three properties that can lead to significant errors. The first of these is the multiplex disadvantage, a property where white or shot noise in the interferogram is spread across all bins in the transform to the spectral domain[3], [4]. Figure 4 shows a contrived example of this phenomenon.

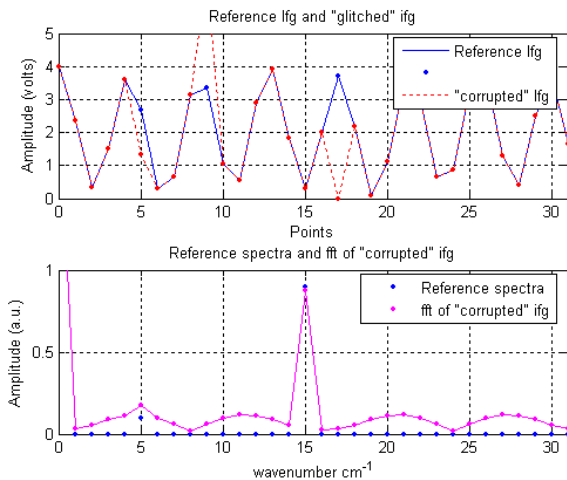


Figure 4: An example of the multiplex disadvantage. The top graph shows a reference interferogram with its corrupted version superimposed. The corresponding spectra are shown in the second graph.

In the top graph, the blue points show an interferogram generated by summing two cosine waves. The first has amplitude of 0.1 (in arbitrary units) at five wavenumbers and

the second has amplitude of 0.9 a.u. at 15 wavenumbers. The super-imposed graph, in red, shows the result when the 6th data word is in error by one-half from its true value. The original 9th and 16th points are multiplied by two to introduce errors at these two points. The resulting spectrum, in figure 4, shows increased amplitude energy at each point of the final spectra.

IV. FFT LEAKAGE

The DFT equation needed to transform data from the spatial to spectral domain is given by:

$$X(k) = \frac{1}{N} \sum_{n=0}^{N-1} x(n) \left[\exp\left(-j\left(\frac{2\pi}{N}\right)kn\right) \right] \quad (3)$$

The inverse transform is given by

$$x(n) = \frac{1}{N} \sum_{k=0}^{K-1} X(k) \left[\exp\left(j\left(\frac{2\pi}{N}\right)kn\right) \right]. \quad (4)$$

Leakage comes when n or k in (3) or (4) is not an integer multiple of the fundamental wavenumber 1/N.

An example of this effect is shown in figure 5.

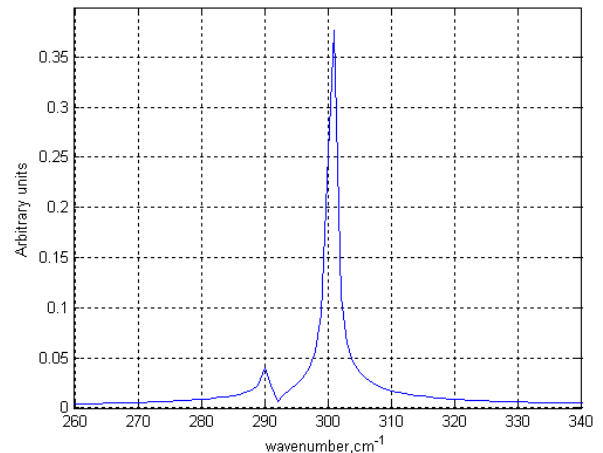


Figure 5: Spectra demonstrating the leakage phenomenon.

The true line spectra, in figure 5, are lines at 290.6 and 300.6 wavenumbers with amplitudes of 0.1 and 1 a.u. respectively. Energy has “leaked” from these wavenumbers into neighboring wavenumbers. This leakage is similar to the

multiplex-disadvantage except the energy is near the parent line spectra and not spread across all wavenumbers.

V. NOISE CONSTRAINTS FOR FFT

Bialkowski [5] states ‘Fourier transform inversion is strictly valid when the noise is stationary or white and errors are normally distributed.’ Although this condition is almost always the case, other probability density functions (pdf) or probability mass functions (pmf) such as Poisson or Cauchy, might be better noise distributions to use in doing EM transforms.

VI. EXPECTATION MAXIMUM TRANSFORM ALGORITHM

The Expectation Maximum (EM) transform is alternate method of performing spectral estimation. Its formulation explicitly addresses the above three disadvantages with the FFT.

The Expectation Maximum algorithm was originally developed in the late 70s and early 80s to reduce emission tomography data [6]-[9]. USU’s Dr. Stephen Bialkowski, from the Department of Chemistry and Biochemistry, has adapted the EM model for use in reducing interferometer data [5].

The desired outcome for the EM algorithm is a best estimate of the object or unobserved spectra distribution, $a(\sigma_j)$ such that $\hat{a}^{(ML)}$, the final spectral estimate, is the optimum image of the true spectra. This maximum likelihood comes when the best description of emission/scattering/reflection of the troposphere, the best detector stochastic properties and the best probability transition description are factored into the EM algorithm.

In the expectation step, the complete data is calculated given the measured interferogram $\bar{y}(d_j)$ and the latest estimate of the optical amplitudes. Summing the complete data over J gives a new expected value for each $\hat{a}(\sigma_j)$. The next step maximizes the likelihood that the difference between the estimated interferogram and the recorded interferogram is minimized. The iterated estimates are given by the following two equations

$$\hat{y}^{(k)}(d_j) = \sum_{i=1}^L p(d_j; \sigma_i) \hat{a}^{(k-1)}(\sigma_i) \quad (5)$$

and

$$\hat{a}^{(k+1)}(\sigma_i) = \frac{\hat{a}^{(k)}(\sigma_i)}{\sum_{j=1}^J p(d_j; \sigma_i)} \frac{\sum_{j=1}^J p(d_j; \sigma_i) \bar{y}(d_j)}{\hat{y}^{(k)}(d_j)} \quad (6)$$

The iteration process starts by setting all spectra bins to unity as an unbiased starting point and computing a first estimate for $\hat{y}^{(k)}(d_j)$ using (5). Given the new estimated interferogram and the raw data vector, $\bar{y}(d_j)$ a new $\hat{a}^{(k+1)}$ vector of I elements is computed. The iterations continue, first (5) and then (6), until a limit is reached or until the metric defined by (7) becomes less than an expected end value.

$$S = \frac{1}{J} \sum_{j=1}^J (\hat{y}(d_j) - \bar{y}(d_j))^2 \quad (7)$$

An example of the iteration process as described by (5) and (6) is given in figure 6.

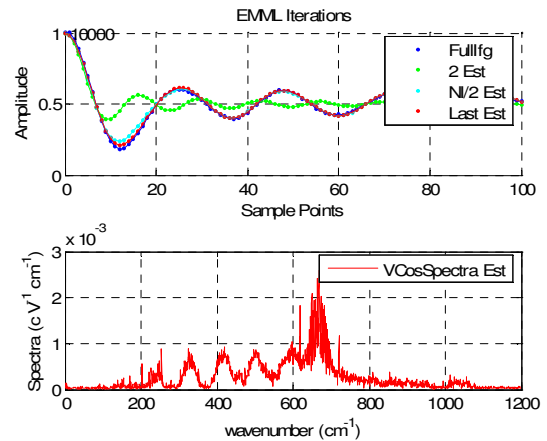


Figure 6: The top panel shows the recorded interferogram and snapshots of the estimated interferogram at different iteration counts. The bottom panel gives the EM spectral estimate.

The top panel shows the estimated interferogram converging towards the observed interferogram as the iterations increase from k =2 to k = 5000, finally stopping at k = 10000 iterations. Note the small change from 5000 to 10000 compared to the change from the second step to 5000 illustrating the iteration becomes asymptotic near the final solution. The bottom panel shows an EM spectral estimate of flight data collected with the sensor looking into deep

space at an altitude of 108,000 feet.

Figure 7 show the EM transform superimposed on the FFT spectra first seen in figure 5. The EM spectrum does not show significant leakage; instead the energy is largely confined to the two lines at 290.6 and 300.6 wavenumbers.

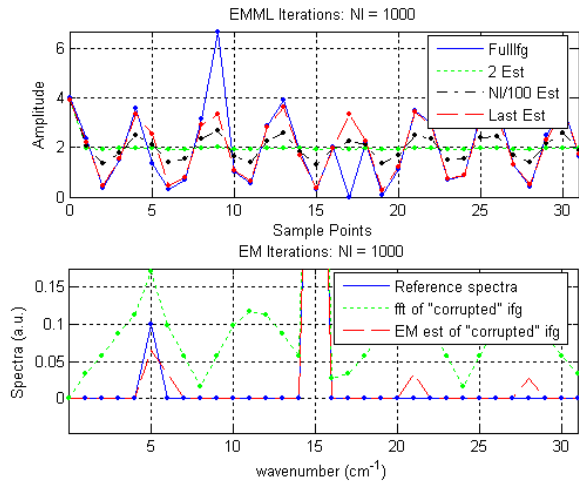


Figure 7: EM transform of ‘corrupted’ interferometric data superimposed on FFT transform.

The graphics in figure 8 show the EM transform of line spectra that are not integer multiple of the fundamental wavenumber. Again the FFT transform shown in figure 5 is also included for reference..

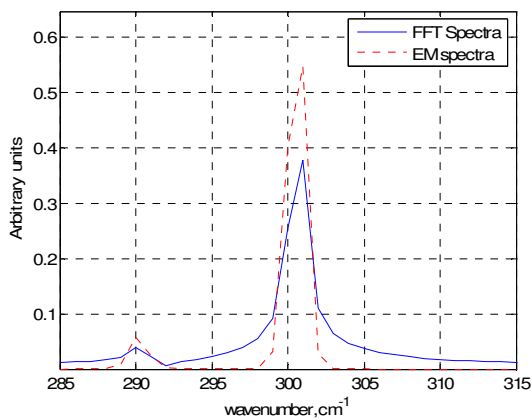


Figure 8: EM spectral estimate superimposed on FFT spectra where the ‘parent’ spectra are a non-integer multiple of the fundamental wavenumber.

VII. CONCLUSIONS AND FUTURE WORK

1) The EM spectral estimation algorithm, described in the paper, shows potential to improve performance in

interferometric data if it is shot noise or quantum-noise limited or if dropouts have occurred.

- 2) The iterative approach, central to the EM transform ,requires significant processing time to yield satisfactory results. Because the process approaches its solution asymptotically, it is difficult to determine when the program has reached a point where further computation can’t improve the result. The example shown in figure 6 was computed at k = 1000 and 10000 steps. S was 0.79 and 0.16, and time was 3.5 and 28.5 minutes respectively. The program now is vector coded into MATLAB[®] giving an improvement of approximately 40 over a ‘for-loop’ implementation. It is estimated C++ code will reduce the computational time by another factor of 10.
- 3) Early data reduction of ideal interferometric data indicates the technique appears to perform best when reducing line spectra. The results are less dramatic for wide-band spectra. Combinations of wide-band and line spectra are yet to be evaluated.
- 4) The algorithm is scheduled to be tested using broadband and line simulated spectra with added white noise distributed using different probability distributions functions. This research will validate and improve the stochastic descriptions of the emission/scatter/reflection and detection processes and improve the estimation of critical spectral features..

REFERENCES

- [1] M. G. Mlynczak, D. G. Johnson, H. Latvakoski, K. Jucks, M. Watson, D. P. Kratz, G. Bingham, W. A. Traub, S. J. Wellard, C. R. Hyde, and X. Liu, “First light from the Far-Infrared Spectroscopy of the Troposphere (FIRST) Instrument,” *Geophysical Research Letters*, Vol. 33, L07704, doi:10.1029/2005GL025114, 2006.
- [2] G. A. Vanasse, A. T. Stair, Jr., D. J. Baker, “*Aspen International Conference on Fourier Spectroscopy*”, 1970.
- [3] J. D. Ingle and S. R. Couch, “*Spectrochemical Analysis* (Prentice Hall, Englewood Cliffs, New Jersey, (1988).
- [4] D R. Fuhrmann, C. Preza, J. A. O’Sullivan, D. L. Snyder, and W. H. Smith, “Spectrum Estimation from Quantum-Limited Interferograms”, *IEEE Transactions on Signal Processing*, Vol. 52, No 4, April 2004.
- [5] S. E. Bialkowski, “Overcoming the Multiplex Disadvantage by Using Maximum-Likelihood Inversion,” *Applied Spectroscopy*, vol. 52, Number 4, pp. 591-598, 1998.
- [6] A. P. Dempster, N. M. Laird, and D. B. Rubin ,J. Roy. Stat. Soc., **B**. 39,1, 1977.
- [7] L.A. Shepp and Y. Vardi, *IEEE Trans.Med.Imag*, **MI-2**, 113, (1982).
- [8] M.I. Miller and D. L. Snyder, *IEEE Proc*, **75**, 892, (1987).
- [9] T. K. Moon and W. C. Stirling, *Mathematical Methods and Algorithms for Signal Processing*, Prentice Hall, Upper Saddle River, NJ, 2000.